



ELSEVIER

19 February 2001

Physics Letters A 280 (2001) 157–161

PHYSICS LETTERS A

www.elsevier.nl/locate/pla

Nonlinear compression of giant surface acoustic wave pulses

A.A. Kolomenskii *, H.A. Schuessler

Texas A&M University, Department of Physics, College Station, TX 77843-4242, USA

Received 6 December 2000; accepted 18 December 2000

Communicated by L.J. Sham

Abstract

The nonlinear propagation of very high-amplitude surface acoustic wave (SAW) pulses in polycrystalline aluminum and copper was studied. A nonlinear compression and an increase of the SAW pulse amplitude have been observed. SAW pulses were numerically simulated with a nonlinear evolution equation including local and nonlocal nonlinear terms. © 2001 Elsevier Science B.V. All rights reserved.

PACS: 62.65.+k; 43.25.+y; 62.20.-x; 68.35.G

Keywords: Nonlinear surface acoustic waves; Nonlinear evolution equation; Pulse compression; Shock front; Laser photoacoustics

1. Introduction

The propagation velocity of high-amplitude acoustic waves depends on the particle velocity of the medium participating in the wave motion. This dependence leads to a nonlinear distortion of the wave profile. For plane bulk waves the evolution of the wave form is described by Burgers equation including one nonlinear term [1] proportional to a nonlinear acoustic constant. In this Letter we consider nonlinear behavior of Rayleigh surface acoustic waves (SAWs) in an isotropic solid. These waves propagate along a free boundary and are localized near the surface decaying inside the solid over a depth of about one wavelength. Nonlinear properties of SAWs gained recently interest in acoustoelectronic applications and seismology [2]. SAWs have two components: one corresponds

to a shear wave with polarization normal to the surface and to the propagation direction (normal component); the other one corresponds to a longitudinal wave and displacements in it are parallel to the unperturbed surface (in-plane component). These two components are connected through boundary conditions and related nonlocally by a Hilbert transform operator. It is noted that Rayleigh SAWs possess no dispersion and therefore efficient interaction of all spectral harmonics takes place during their propagation. The nonlinearity of the medium causes changes in the waveform of one component which depend also on the nonlinear interaction with the other component. As a result, for the description of the SAW nonlinearity, besides the usual local nonlinear term encountered in Burgers equation, also nonlocal terms should be taken into account [3–5]. In order to describe the nonlinear propagation of a SAW in an isotropic solid three nonlinear acoustic constants must be introduced [5]: one constant of the local nonlinearity and two constants of the nonlocal nonlinearity. The explicit expressions for these constants [6] reveal that two of them depend on

* Corresponding author. Tel.: (979)-845-7861, fax: (979)-845-2590.

E-mail address: a-kolomenski@physics.tamu.edu (A.A. Kolomenskii).

the nonlinear elastic moduli of the third order, which describe the nonlinear behavior of the material. One constant of the nonlocal nonlinearity depends only on the elastic moduli of the second order. Thus, measurements of the nonlinear propagation of SAWs and the determination of nonlinear acoustic constants can provide two relationships for the determination of the third-order elastic moduli and characterization of the nonlinear elastic properties of the solid.

Recently, it was experimentally demonstrated [7,8] that SAW pulses propagating in fused quartz (Herasil) experience nonlinear extension and two shock fronts can be formed in the in-plane surface velocity of a SAW pulse corresponding to two sharp peaks in the normal surface velocity. Here we report a qualitatively different nonlinear behavior observed in polycrystalline aluminum and copper. In these materials a compression of the central part of the pulse takes place. By comparing our results with calculations based on the nonlinear evolution equation [5,7] we show that the observed compression or extension of the SAW pulse depends on the sign of the nonlinear acoustic constant determining the action of the local nonlinearity.

2. Experimental setup

The SAW pulses were excited by nanosecond pulses of a Nd:YAG laser with a pulse duration 26 ns and energy 100 mJ. The excitation region was covered with a layer of aqueous carbon suspension of thickness $d \sim 50 \mu\text{m}$. This layer had a high absorption coefficient ($\sim 300 \text{ cm}^{-1}$) and provided efficient conversion of the energy of the laser pulse into the energy of elastic stresses and the SAW wave motion. To additionally enhance the pressure acting onto the surface of the sample a glass plate with a thickness of 3 mm was placed on top of the absorption layer. This plate confined the overheated medium allowing a significant increase of the mechanical stresses created in the interaction region, which consequently resulted in much higher amplitudes of the excited SAW pulses. The laser radiation was sharply focused onto the surface of the specimen in a strip of $\sim 8 \text{ mm}$ long and $\sim 10 \mu\text{m}$ wide near the edge of the absorption layer covered with the glass plate. This was necessary to produce a high-amplitude short SAW pulse and to

avoid its strong absorption during propagation under the plate.

A SAW pulse propagated perpendicular to the excitation strip and was detected at two spots along the track by a probe-beam deflection setup with nanosecond resolution. The setup was calibrated for each measurement, so that the registered signal allowed to determine both the temporal shape and the amplitude of the normal surface velocity. The distance between the source and the spots could be adjusted. Each measurement was performed with a single laser pulse.

3. Theoretical model

An estimate of the pressure produced on the surface with the laser fluence of $F \sim 100 \text{ J/cm}^2$ used in our experiments gives $p = GF/d \sim 2 \text{ GPa}$, where $G \sim 0.1$ is the Grueneisen parameter for water. According to the theoretical treatment [9] such high-amplitude transient pressure pulses produce SAW pulses with an acoustic Mach number of $M \sim 0.01$ in agreement with our experimental results presented below.

For theoretical description of the SAW pulse propagation we used the nonlinear evolution equation [5] derived under the assumption that the temporal and spatial changes of the SAW waveform are small on the scale of the pulse duration and characteristic wavelength. The equation for the in-plane surface velocity component v of the SAW pulse propagating along the x -axis in an isotropic solid can be presented in the form

$$\begin{aligned} \frac{\partial v}{\partial x} - \varepsilon_1 c_R^{-2} v \frac{\partial v}{\partial \tau} - \delta \frac{\partial^2 v}{\partial \tau^2} \\ = \frac{\varepsilon_2 c_R^{-2}}{2} \frac{\partial}{\partial \tau} \{v^2 + (H[v])^2\} \\ + \varepsilon_3 c_R^{-2} \left\{ v \frac{\partial v}{\partial \tau} + H \left[v H \left[\frac{\partial v}{\partial \tau} \right] \right] \right\}, \end{aligned} \quad (1)$$

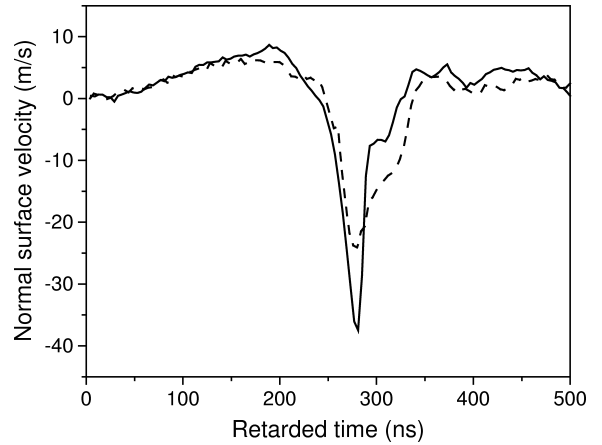
where $\tau = t - x/c_R$ is the retarded time and c_R is the propagation velocity of the Rayleigh SAW. It is assumed that the solid is infinitely thick and occupies a half-space $z \leq 0$. The expression on the left-hand side of the equation is known from the theory of nonlinear bulk acoustic waves as Burgers operator [10]. It takes into account the local nonlinearity proportional

to ε_1 and attenuation proportional to the coefficient δ . The two terms on the right-hand side are proportional to the nonlinear acoustic constants $\varepsilon_2, \varepsilon_3$ and are non-local since they contain the integral Hilbert transform operator $H[v] = \pi^{-1} P V \int_{-\infty}^{+\infty} v(\tau')(\tau' - \tau)^{-1} d\tau'$. The nonlocal terms describe the interaction of the in-plane v and the normal v_n components of the surface velocity. These components are related through the expressions $v_n = \gamma^{-1} H[v]$ and $v = -\gamma H[v_n]$, where γ is a dimensionless combination of the bulk and surface acoustic velocities of the solid [9].

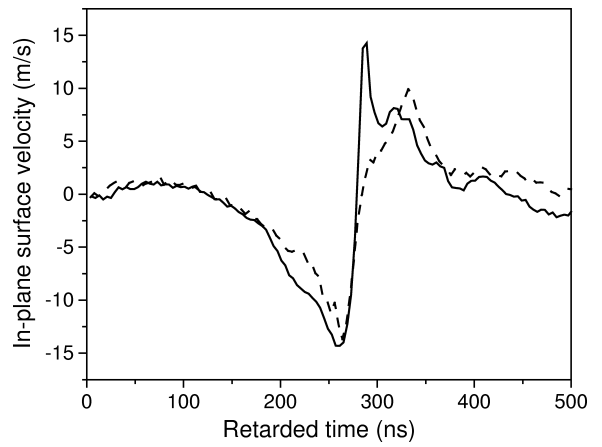
4. Results and discussion

In Fig. 1(a) the waveforms of the normal surface velocity detected in aluminum at two distances $x_1 = 13.8$ mm and $x_2 = 26.4$ mm are shown. The corresponding in-plane components were calculated for each waveform using Hilbert transform and are presented in Fig. 1(b). At a smaller distance the FWHM duration of the central negative peak of the normal surface velocity is $\tau_1 = 50$ ns and at the larger distance it is $\tau_2 = 22$ ns. The amplitudes of the surface velocity and the acoustic Mach numbers are $v_1 = 10$ m/s, $M_1 = v_1/c_R = 3.4 \times 10^{-3}$, $v_{n1} = 24$ m/s, $M_{n1} = v_{n1}/c_R = 8.2 \times 10^{-3}$ and $v_2 = 15$ m/s, $M_2 = v_2/c_R = 5.2 \times 10^{-3}$, $v_{n2} = 38$ m/s, $M_{n2} = v_{n2}/c_R = 1.3 \times 10^{-2}$, respectively. Thus, the central part of the pulse experiences a nonlinear compression in the propagation process.

In Fig. 2 the results of numerical simulations are presented. It is assumed in the calculation that the initial pulse shape is provided by the waveform at the first distance and the waveform at the second distance is calculated with the evolution equation (1). The values of the nonlinear acoustic parameters $\varepsilon_1 = 0.88$, $\varepsilon_2 = -1.0$, $\varepsilon_3 = 4.0$ are calculated from the third-order nonlinear elastic moduli [11] according to explicit formulas for these parameters [6]. The attenuation constant $\delta \sim 2.4 \times 10^{-16}$ s²/cm and SAW velocity $c_R = 2910$ m/s are determined from measurements of low-amplitude pulses at two propagation distances; $\gamma = 1.58$ is used in numerical simulations for polycrystalline aluminum. Eq. (1) approximates attenuation by a quadratic frequency dependence, which is reasonable for polycrystalline metals in the frequency range of interest from 2 to 100 MHz [12]. The solid



(a)



(b)

Fig. 1. Waveforms of giant SAW pulses observed in aluminum at two propagation distances $x_1 = 13.8$ mm (dashed lines) and $x_2 = 26.4$ mm (solid lines) showing the nonlinear evolution of the pulse shape: (a) normal surface velocity, (b) in-plane surface velocity.

lines in Figs. 2(a) and (b) show the normal and in-plane surface velocities in the SAW pulse calculated with the evolution equation (1) when all three parameters $\varepsilon_{1,2,3}$ are taken into account. For convenience of comparison the experimentally determined waveforms at the second distance are shown by crosses.

It should be noted that the solutions of Eq. (1) and their features distinguishing them from those of the Burgers equation are not well studied so far. The solutions of Burgers equation (left-hand side of Eq. (1),

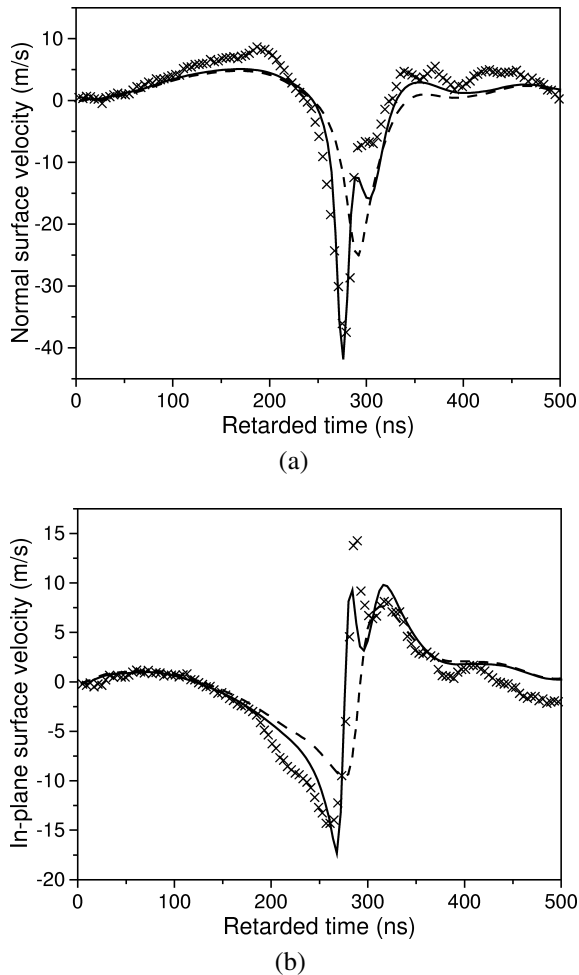


Fig. 2. Calculated waveforms of SAW pulses: (a) normal surface velocity, (b) in-plane surface velocity. Solid lines were calculated with both local and nonlocal nonlinearities taken into account ($\varepsilon_1 = 0.88$, $\varepsilon_2 = -1.0$, $\varepsilon_3 = 4.0$); the dashed lines were obtained with the local nonlinearity only ($\varepsilon_1 = 0.88$, $\varepsilon_2 = 0$, $\varepsilon_3 = 0$). For convenience of comparison experimentally determined waveforms are shown by crosses.

when only local nonlinearity is taken into account, i.e., $\varepsilon_2 = \varepsilon_3 = 0$) are shown for comparison in Figs. 2(a) and (b) by dashed lines. The substantial difference of the solutions in these two cases demonstrates that the nonlocal terms are rather important for quantitative analysis. In particular, the increase of the amplitude, the temporal shift of the shock front, and a cuspidal shape of the positive and negative peaks of the in-plane surface velocity result from the nonlocal nonlinearity.

Nevertheless, it can be seen that the SAW pulse compression effect takes place even when $\varepsilon_2 = \varepsilon_3 = 0$. Therefore qualitative conclusions can also be derived from the known properties of the solutions of Burgers equation. Specifically, let us consider the in-plane components shown in Fig. 1(b). It is known for solutions of Burgers equation that a point of the pulse profile with the medium velocity v propagates (before the shock front was formed) with the velocity $c_R + \varepsilon_1 v$ [10]. Thus, for a negative portion of the pulse and a positive parameter ε_1 (as we have for aluminum) the propagation velocity is lower than c_R . For a positive portion of the pulse the propagation velocity is higher than c_R . Thus, positive and negative peaks of the pulse profile approach each other during the pulse propagation forming a steep shock front in the in-plane surface velocity and corresponding narrow negative peak in the normal surface velocity.

A qualitatively different behavior was observed in fused quartz (Herasil) [7,8], which has negative value of the parameter of the local nonlinearity, $\varepsilon_1 \approx -1$. In this material positive and negative peaks of the in-plane velocity waveform of a high-amplitude SAW pulse move away from each other and, consequently, two shock fronts, one in the head and another in the tail of the SAW pulse can be formed in this case.

The compression of the SAW pulse corresponds to frequency up-conversion processes resulting in an increase of the spectral amplitudes in the high-frequency domain. In polycrystalline metals high-frequency spectral components experience a rather strong attenuation. In materials with small attenuation of SAWs such frequency up-conversion can be used to advance the spectral content into gigahertz and even terahertz frequency ranges.

The observed property of the nonlinear compression of high-amplitude SAW pulses is not unique for polycrystalline aluminum. We observed a similar effect in polycrystalline copper (Fig. 3). The SAW pulses have the following parameters: at $x_1 = 6.7$ mm the values are $v_1 = 7.5$ m/s, $M_1 = 3.5 \times 10^{-3}$, $v_{n1} = 14$ m/s, $M_{n1} = 6.5 \times 10^{-3}$, and at $x_2 = 19.9$ mm the values are $v_2 = 8.5$ m/s, $M_2 = 4.0 \times 10^{-3}$, $v_{n2} = 15$ m/s, $M_{n2} = 7.0 \times 10^{-3}$. In Fig. 3 the solid line shows the result of a numerical simulation with the nonlinear acoustic parameters $\varepsilon_1 = 1.0$, $\varepsilon_2 = -0.98$, $\varepsilon_3 = 4.1$, evaluated from the elastic moduli of the third order [11]. The values of other parameters used for copper are $\gamma = 1.57$,

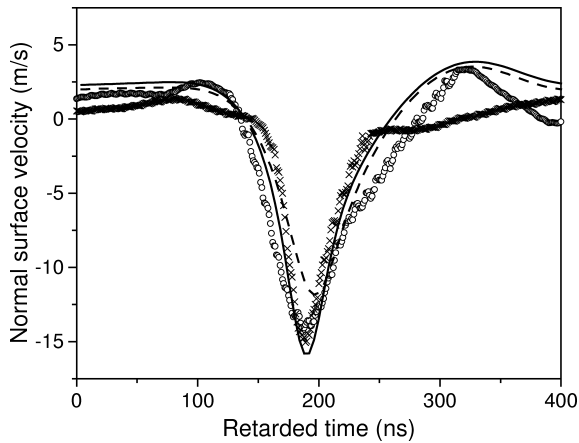


Fig. 3. Waveforms of the normal surface velocity in a nonlinear SAW pulse measured in copper at two distances $x_1 = 13.9$ mm (open circles) and $x_2 = 26.7$ mm (crosses) from the source. The solid line shows the result of the calculation with the evolution equation (1) and $\varepsilon_1 = 1.0$, $\varepsilon_2 = -0.98$, $\varepsilon_3 = 4.1$; the dashed line shows the calculation result with the local nonlinearity only ($\varepsilon_1 = 1.0$, $\varepsilon_2 = 0$, $\varepsilon_3 = 0$).

$c_R = 2150$ m/s, and $\delta \sim 2.4 \times 10^{-16}$ s²/cm. It should be noted that in numerical simulation for periodic SAWs in steel [4] a formation of a narrow negative peak in the normal surface velocity was also obtained.

In conclusion, we have studied the nonlinear behavior of high-amplitude SAW pulses in polycrystalline metals (aluminum and copper). A compression of the central part of the pulse and formation of one shock front was registered in these solid materials. This nonlinear behavior is qualitatively mainly determined by the positive parameter ε_1 responsible for the local nonlinearity, although nonlocal nonlinearity also changes significantly the amplitude and the shape of SAW

pulses. Good agreement was obtained with model calculations based on the nonlinear evolution equation with three nonlinear acoustic constants that were determined from the third-order elastic moduli.

Acknowledgements

We thank S. Zhrebtssov for assistance in the construction of the setup. Support from NSF (grants 9870143 and 9970241) is gratefully acknowledged.

References

- [1] J.M. Burgers, *Adv. Mech.* 1 (1948) 1.
- [2] A.P. Mayer, *Phys. Rep.* 256 (1995) 237.
- [3] D.F. Parker, F.M. Talbot, *J. Elast.* 15 (1985) 389.
- [4] E.A. Zabolotskaya, *J. Acoust. Soc. Am.* 91 (1992) 2569.
- [5] V.E. Gusev, W. Lauriks, J. Thoen, *Phys. Rev. B* 55 (1997) 9344.
- [6] V.E. Gusev, W. Lauriks, J. Thoen, *J. Acoust. Soc. Am.* 103 (1998) 3203.
- [7] A.A. Kolomenskii, A.M. Lomonosov, R. Kuschnerit, P. Hess, V.E. Gusev, *Phys. Rev. Lett.* 79 (1997) 1325.
- [8] A. Lomonosov, V.G. Mikhalevich, P. Hess, E. Yu. Knight, M.F. Hamilton, E.A. Zabolotskaya, *J. Acoust. Soc. Am.* 105 (1999) 2093.
- [9] A.A. Kolomenskii, A.A. Maznev, *Sov. Phys. Acoust.* 36 (1990) 463.
- [10] O.V. Rudenko, S.I. Soluyan, *Theoretical Foundations of Nonlinear Acoustics*, Consultants Bureau, New York, 1977.
- [11] Landolt-Boernstein: *Numerical Data and Functional Relationships in Science and Technology*, New Series, Group 3, Vol. 7, Springer, Heidelberg, 1984.
- [12] E.P. Papadakis, in: W.P. Mason (Ed.), *Physical Acoustics*, Vol. 4, Academic Press, New York, 1968, Part B.